

Domain size effects in Barkhausen noise

M. Bahiana and Belita Koiller
Instituto de Física, UFRJ, Rio de Janeiro, RJ, Brazil

S. L. A. de Queiroz
Instituto de Física, UFF, Niterói, RJ, Brazil

J. C. Denardin and R. L. Sommer
Departamento de Física, UFSM, Santa Maria, RS, Brazil
 (Received 16 July 1998)

The possible existence of self-organized criticality in Barkhausen noise is investigated theoretically through a single interface model, and experimentally from measurements in amorphous magnetostrictive ribbon Metglas 2605TCA under stress. Contrary to previous interpretations in the literature, both simulation and experiment indicate that the presence of a cutoff in the avalanche size distribution may be attributed to finite-size effects. [S1063-651X(99)00904-6]

PACS number(s): 05.40.-a, 75.60.Ej, 68.35.Rh

The Barkhausen effect consists of magnetic noise caused by erratic jumps in the magnetization of a ferromagnetic material, under an increasing applied magnetic field [1]. A simple explanation for this effect is the combination of random pinning of domain walls by defects and the driving external field, which is essentially the same mechanism present in stick-slip processes [2]. Recently the statistical behavior of Barkhausen noise has attracted much interest, due to the possibility of providing an experimental realization of self-organized critical (SOC) behavior [3–5]. The subject is controversial, however. We concentrate here on the results obtained by Urbach, Madison, and Markert (UMM) [4] and Perković, Dahmen, and Sethna (PDS) [5].

UMM measured the avalanche size probability distribution function in an Fe-Ni-Co alloy, and found power-law decay over approximately two decades, followed by an exponential cutoff. The same result was also observed in numerical simulations of the interface motion. The power-law behavior, obtained without any intentional fine tuning of parameters, suggests that this system self-organizes into a critical state. On the other hand, PDS argued that such behavior can be explained without recourse to SOC concepts: in their view, the power-law decay followed by a cutoff is evidence that the system is *near* but not quite *at* a conventional critical point. They performed simulations for the random-field Ising model (RFIM) under an external field, taking the local (pinning) fields to be Gaussian disordered with standard deviation R . The avalanche-size distribution is also characterized by a power law followed by a cutoff, and the power-law regime increases over several decades as R approaches a critical disorder R_C .

Although UMM and PDS approach the problem with apparently similar models, their conclusions regarding the critical nature of the Barkhausen noise are in contradiction. Here we show that in reality, the ingredients used in either model differ in crucial aspects where the onset of SOC is concerned, so it is not surprising that they end up with different findings.

We investigate this question by using the simple model proposed by UMM [4] for the motion of a single domain wall in the Barkhausen noise regime. We find that the existence of a cutoff in the UMM model can be traced back to finite-size effects; experimental results, also to be described, bear out the idea that the cutoff to be found there originates from corresponding aspects in real systems.

In UMM's model, the interface at time t is described, in space dimensionality d , by its height $h(\vec{\rho}_i, t)$, where $\vec{\rho}_i$ is the position vector of site i in a $(d-1)$ -dimensional lattice. At each t , the height function $h_i = h(\vec{\rho}_i, t)$ is assumed to be single valued, so there are no overhangs on the interface. Thus the interface element corresponding to the d -dimensional position vector $\vec{r}_i = (\vec{\rho}_i, h_i)$ may be unambiguously labeled i . Simulations are performed on a $L^{d-1} \times \infty$ geometry, with the interface motion set along the infinite direction. Therefore finite-size effects are controlled by the length parameter L . Each element i of the interface experiences a force of the form

$$f_i = u(\vec{r}_i) + \frac{k}{z} \left[\sum_{j=1}^z h_{l_j(i)} - z h_i \right] + H_e, \quad (1)$$

where

$$H_e = H - \eta M. \quad (2)$$

The first term on the RHS of Eq. (1) represents the pinning force, u , and brings quenched disorder into the model by being chosen randomly, for each lattice site \vec{r}_i , from a Gaussian distribution of zero mean and standard deviation R . Large negative values of u lead to local elements where the interface will tend to be pinned, as described in the simulation procedure below. The second term corresponds to a cooperative interaction among interface elements, assumed here to be of elastic (surface tension) type. In this term $l_j(i)$ is the position of the j th nearest neighbor of site i and z is the coordination number of the $(d-1)$ -dimensional lattice over

which the interface projects. The tendency of this term is to minimize height differences among interface sites: higher (lower) interface elements experience a negative (positive) force from their neighboring elements. The force constant k gives the intensity of the elastic coupling, and is taken here as the unit for f . The last term is the effective driving force, resulting from the applied uniform external field H and a demagnetizing field which is taken to be proportional to $M = (1/L^{d-1})\sum_{i=1}^{L^{d-1}} h_i$, the magnetization of the previously flipped spins for a lattice of width L .

Other models discussed in the literature [5–7] have the same basic ingredients described in Eq. (1), namely, local quenched disorder, a cooperative term, and a driving field. In the RFIM, for example, the cooperative term is not elastic, but is driven by nearest-neighbor exchange interactions [5]. Accordingly, power-law distributions are usually obtained along several decades of avalanche sizes; however, the question of whether an SOC-like mechanism is present is an altogether different matter. What is essential for SOC is that no fine tuning of parameters be required to keep the system at a critical state. Such a distinction is clearly illustrated in Ref. [4], where several variants of the present model were introduced. It was established that even without including any demagnetizing effect at all, a power-law distribution of avalanche sizes would arise if the external field were kept close to its (sharply defined) critical value for interface depinning. Including a demagnetizing field proportional to the local magnetization did away with fine tuning: rather, the effective field $H - \eta M$ was seen to stay approximately constant as H and consequently M increased. Even then, the negative auto-correlation between avalanche sizes at short times (observed in experiments, and also believed to be an essential feature in the theory of SOC) only arose in simulations when the *global* magnetization term H_e shown in Eq. (2) was considered. Given the established adequacy of the UMM model to describe SOC-like aspects of experiments, we concentrate our simulations in that same model.

We start the simulation with a flat wall and zero applied field. All spins above it are unflipped. The force f_i is then calculated for each site, and each spin at a site with $f_i \geq 0$ flips, causing the interface to move up one step. The magnetization is updated, and this process continues until $f_i < 0$ for all sites, when the interface comes to a halt. The external field is then increased by the minimum amount needed to bring the most weakly pinned element to motion. The avalanche size corresponds to the number of spins flipped between two interface stops. The field value can be used as a time scale (the only relevant one in the case). This mimics the experimental setup of a linearly increasing field during the data acquisition interval (one might as well use the accumulated number of interface stops as a surrogate time scale; we did both, with the same qualitative results). As in UMM [4], we are implicitly assuming that the experimental situation simulated is one of sufficiently slow driving rate, such that avalanches do not overlap.

Our simulations have been conducted in $d=2$ and $d=3$, in square and cubic space lattices respectively. Here we concentrate on the three-dimensional (3D) results. After a transient, the effective field always settles onto a critical value H_c which depends on R , k , and η . The fact that the system tunes itself to a constant effective field is in itself an indica-

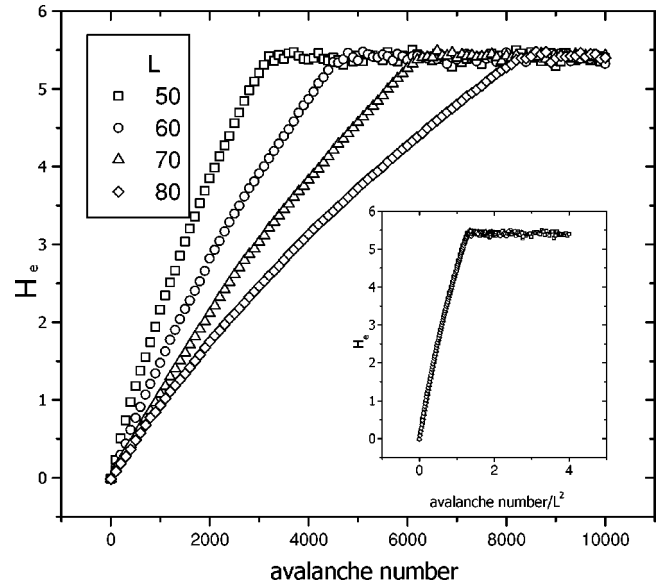


FIG. 1. Simulation on a 3D lattice for systems with $R=5.0$, $k=1$, $\eta=0.05$, and different widths. Starting the external field at $H=0$, the effective field H_e grows linearly and saturates at a critical value after a transient. Here we see this behavior as a function of the avalanche number and, in the inset, the same but with avalanche number scaled by L^2 .

tion of SOC-like behavior. If the external field is started at a higher value, a large avalanche occurs and brings the effective field back to the adequate value. On the other hand, if the field starts from zero there is a transient corresponding to a series of small avalanches. We find that the number of avalanches in this transient is proportional to L^{d-1} . This means that an infinite system would need an infinite number of avalanches to reach criticality. As an illustration of this behavior, we present in Fig. 1 the effective field in a 3D system for $R=5.0$, $k=1$, and $\eta=0.05$ for different simulation cell sizes L .

The calculated avalanche-size distribution corresponds to a power law with a cutoff, as obtained by UMM in Barkhausen experiments and in simulations [4], and also by PDS [5] within their RFIM model. It was shown in the latter reference that the cutoff is intrinsic to the RFIM, if the system is away from the critical point R_c . In what follows we present evidence that the nature of the cutoff in the Barkhausen effect, both in simulations of the Urbach model and in experiments, is a finite-size effect. The characterization of the cutoff as a finite-size effect was recently suggested by Narayan [8] through the analysis of a continuum model closely based on UMM's, though no attempt was made there to quantify the relationship. We have examined the dependence of the cutoff on the simulation cell size L by collecting a series of 100 000 avalanches for $L=50, 80, 150, 200$, and 400. Figure 2 shows the avalanche size distribution for some values of L in 3D lattices. The transient was eliminated by starting the external field near H_c . We can clearly see that the cutoff shifts to higher values of A with increasing L . Following the standard procedure [4,5,7] we seek for a signature of SOC in a power-law distribution of avalanche sizes; on top of this, the cutoff must be accounted for, which we do phenomenologically via a simple exponential tail [9]: Thus, the histograms were fitted by the function $P(A)$

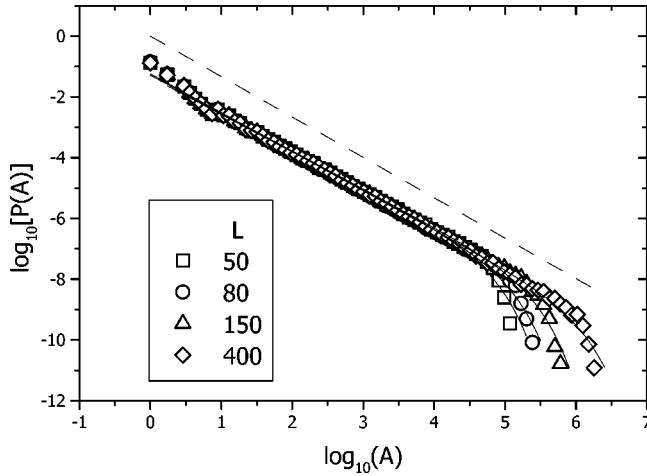


FIG. 2. Avalanche size distribution calculated from simulations for $R=5.0$, $k=1$, $\eta=0.05$, and the indicated values of lattice widths L , in 3D. Thin solid lines are fits to the form $P(A) \propto A^{-\alpha} \exp(-A/A_0)$ with α between 1.23 and 1.35 and A_0 , the cut-off size, increasing as a power of L (see text). The dashed line has slope -1.3 , for comparison with UMM's experimental data.

$\propto A^{-\alpha} \exp(-A/A_0)$ with α in the range $(1.23 \pm 0.02 - 1.35 \pm 0.02)$. The parameter A_0 , which defines the cutoff size, is strongly dependent on L : $A_0 \propto L^{1.4 \pm 0.1}$. We have also varied the disorder parameter R , in an attempt to find an effect similar to that described by PDS in their RFIM model. However, the final picture was qualitatively always the same as shown in Fig. 2, with roughly the same power-law dependence of A_0 on L . In $d=2$ we used lattices of width $L = 100, 500, 1000, 2000, 3000$, and 5000 from which a value of $\alpha = 0.83 \pm 0.08 - 1.03 \pm 0.03$ and $A_0 \propto L^{0.78 \pm 0.06}$ were obtained. Thus, we conclude that the presence of a cutoff in the avalanche size histogram is a finite-size effect. Though it may seem puzzling that the finite *transverse* dimensions can influence the characteristics of interface motion along the *unbound* direction of growth, a qualitative picture of the corresponding mechanism is as follows. Each time the $(d-1)$ -dimensional lattice is swept, the number of distinct chances for the interface to move is of order $N \sim L^{d-1}$; thus, if the typical probability for a given interface element not to advance (that is, to have $f_i < 0$) is p , the interface as a whole will come to a halt, marking the end of an avalanche, only if $f_i < 0$ for *all* elements. This happens with probability p^N , hence for large L larger avalanches become more probable.

The above result clearly demonstrates the different nature of the cutoff in the UMM and PDS simulation models. Both models describe domain walls advancing in a disordered magnetic medium: The key difference between them is the presence of a demagnetizing field, proportional to the growing domain magnetization. This field is an essential element to bring the simulations into an SOC regime.

Although variations in L are easily accessible in simulations, this is not a trivial parameter to vary in experiments. For magnetic systems, one would expect L to be related to the typical magnetic domain size in a sample. Magnetic materials have the interesting property of magnetostriction, which is the change in internal domain configurations as a response to applied anisotropic stress. Positive magnetostrictive materials show an increase in internal domain wall

lengths under applied stress [10], and may therefore be employed in investigating experimentally L -dependent effects in Barkhausen noise experiments. We performed measurements in a disordered material with this property, namely amorphous magnetostrictive ribbon Metglas 2605TCA under stress σ . Different stress values were applied in order to increase domain wall length, as seen in Ref. [10]. Stress is expected also to change the domain wall thickness $\delta = \sqrt{\mathcal{A}/K_\sigma}$, where \mathcal{A} is the effective exchange constant, $K_\sigma = \frac{3}{2} \lambda_S \sigma$ and $\lambda_S = 27 \times 10^{-6}$ is the saturation magnetostriction constant for this material. In amorphous materials, fluctuations in the stress due to local composition fluctuations generate the pinning sites for domain walls. Their magnitudes are much larger than those originated from the external forces. Thus, the effect of the applied stresses will be to order the domain wall structure by changing the domain size and length. The magnetoelastic anisotropy, on the other hand, tends to stretch existing domain walls [10].

Metglas 2605TCA samples ($80 \text{ mm} \times 1 \text{ mm} \times 30 \mu\text{m}$) were preannealed in an Ar flow at 300°C for 15 min in order to decrease the stress level associated with the fabrication process. The measurements were performed in an open magnetic circuit. As a consequence, there is a global effective field acting on the domain walls; also, the average magnetization rate $\dot{M}(t)$ and differential susceptibility were kept constant. The samples were cycled in their hysteresis loops, excited by a slowly varying (triangular, 0.2 Hz, 4 Oe maximum value) field. The Barkhausen signal was detected by a small coil ($5 \text{ mm} \times 1 \text{ mm} \times 0.5 \text{ mm}$) tightly wound around the central part of the sample. Thus, the cross-section of the coil was rectangular, approximately following the external contour of the sample's cross section. The signal was preamplified by a SR550 low pass amplifier and digitized by a TDA320 oscilloscope. The low pass amplifier was set to an upper frequency limit equal to half the sampling frequency of 20 kHz. The wave-form generator, current source, and preamp were fed by batteries in order to increase the signal to noise ratio. At each cycle and starting from a given value of a trigger field, a time series was acquired (in a total of 150 for each stress value) and stored for further processing. For each stress level, we identify an avalanche with a jump in the voltage level V . As in Ref. [4], a threshold voltage was established according to experimental resolution, which defines the low-end cutoff of the measured avalanche distribution. Note, however, that our main concern here is with the statistics of the largest avalanches, which will be sensitive to finite-size effects.

The avalanche (voltage jump) size distributions were obtained for $\sigma = 0, 17, 30, 80, 100, 150, 180, 230, 300, 400$, and 525 MPa . In order to obtain such distributions, a total of 7000 jumps were used for each value of applied stress. Some of these results are shown in Fig. 3. One must note that, especially for low-stress data, the combination of experimental resolution available and the intrinsic characteristics of Metglas resulted in a rather narrow power-law region, spanning at most a decade and a half (for the highest applied stress, 525 MPa). This is to be compared e.g., with two decades in UMM's single experimental result [4]. Bearing in mind that the reliability of numerical analyses of our data is therefore limited, one still can see some unequivocally de-

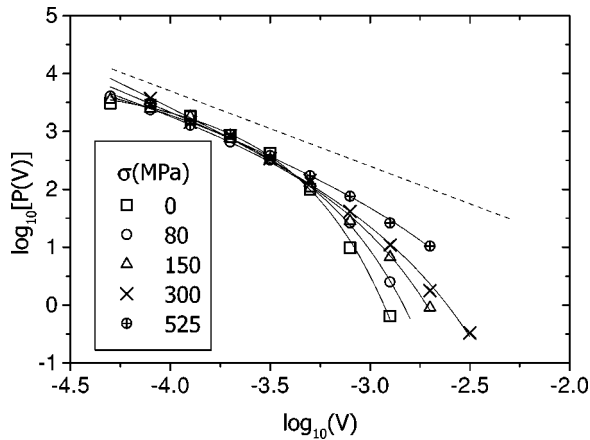


FIG. 3. Histogram of voltage jumps for different values of applied stress σ . Thin solid lines are fits to the form $P(V) \propto V^{-\alpha} \exp(-V/V_0)$ with α between 0.29 and 1.6 and V_0 , the cutoff voltage, increasing as a power of σ (see text). The dashed line, included for comparison with Fig. 2 and with UMM's experimental data, has the same slope as the dashed line there, -1.3 .

finer trends. The main point to be taken is that the cutoff clearly increases with the applied stress. Since stress increases the magnetic domains, what we see here is again the dependence of the cutoff on a typical domain size, in accordance with the simulation results. We fitted our experimental histograms with the function $P(V) \propto V^{-\alpha} \exp(-V/V_0)$. As expected from our relatively narrow effective resolution, this yielded quite a large spread in the fitted values of α , which turned out to be in the range $0.29 \pm 0.1 - 1.6 \pm 0.1$ (central

estimates increasing, and relative error bars narrowing, with increasing applied stress). However, the growing trend of the cutoff against stress comes out clearly enough as $V_0 \propto \sigma^{(0.65 \pm 0.04)}$. The fact that experimental values of α fall in a similar range to those from the 3D simulations is both to be expected and in line with the earlier results of UMM. On the other hand, the power that governs the dependence of A_0 on σ need not coincide with that which relates A_0 to L in the numerical work. In order to predict a relationship between the two quantities, one would need to work out the connection of the physical mechanisms driving the interplay between finite transverse dimensions and avalanche sizes, in the interface model, to the corresponding ones between applied stress and domain wall length in actual samples. So far, we have not been able to do this.

From the above results we conclude that the cutoff in the avalanche size histogram in Barkhausen systems is a finite-size effect. This, together with the presence of a self-tuning effective field and negative time correlation for short times, is a strong indication that SOC is present. Also, we find that any attempt to model Barkhausen noise must necessarily include the demagnetizing field, for this is the key ingredient for the above mentioned self-tuning.

Note added. Recently, we became aware of similar work (e-print cond-mat 9808224) on samples of $\text{Fe}_{64}\text{Co}_{21}\text{B}_{15}$ under stress, where $V_0 \sim \sigma^{0.5}$ is found. We thank G. Durin and S. Zapperi for interesting correspondence.

This work was partially supported by CNPq, CAPES, and FAPERGS (Brazil). We thank M. Novak, J. Urbach, and A. Hansen for interesting discussions.

[1] H. Barkhausen, Phys. Z. **20**, 401 (1919).
 [2] H. J. S. Feder and J. Feder, Phys. Rev. Lett. **66**, 2669 (1991).
 [3] K. P. O'Brien and M. Weissman, Phys. Rev. E **50**, 3446 (1994).
 [4] J. Urbach, R. Madison, and J. Markert, Phys. Rev. Lett. **75**, 276 (1995).
 [5] O. Perković, K. Dahmen, and J. Sethna, Phys. Rev. Lett. **75**, 4528 (1995).
 [6] H. Ji and M. O. Robbins, Phys. Rev. A **44**, 2538 (1991).
 [7] P. Cizeau, S. Zapperi, G. Durin, and H. Stanley, Phys. Rev. Lett. **79**, 4669 (1997).

[8] O. Narayan, Phys. Rev. Lett. **77**, 3855 (1996).
 [9] The power law behavior with an exponential cutoff for the Barkhausen effect curves has been derived in the literature for some special cases [see, for example, B. Alessandro *et al.*, J. Appl. Phys. **68**, 2901 (1990)]. It was explicitly adopted in Ref. [4], and appears to have been used in Ref. [5] for the fits in their Fig. 1. This is the simplest form one could devise for the fitting.
 [10] K. Yamamoto, T. Sasaki, and Y. Yamashiro, J. Appl. Phys. **81**, 5796 (1997).